Bioorganic Chemistry 90 (2019) 103042

Contents lists available at ScienceDirect

Bioorganic Chemistry

journal homepage: www.elsevier.com/locate/bioorg

Green synthesis of selenium-*N*-heterocyclic carbene compounds: Evaluation of antimicrobial and anticancer potential

Amna Kamal[a], Mansoureh Nazari V.[b], Muhammad Yaseen[d], Muhammad Adnan Iqbal[a,c,*], Mohamed B. Khadeer Ahamed[e], Aman Shah Abdul Majid[f], Haq Nawaz Bhatti[a]

[a] Department of Chemistry, University of Agriculture, Faisalabad 38040, Pakistan
[b] Department of Pharmacology, School of Pharmaceutical Sciences, Universiti Sains Malaysia, Minden, 11800 Pulau Penang, Malaysia
[c] Organometallic and Coordination Chemistry Laboratory, Department of Chemistry, University of Agriculture, Faisalabad 38040, Pakistan
[d] Department of Chemistry, University of Education (Lahore), Faisalabad Campus, Faisalabad, Pakistan
[e] EMAN Biodiscoveries Sdn. Bhd., A1-4, Lot 5, Persiaran 2/1, Kedah Halal Park, Kawasan Perindustrian Sungai Petani, 08000 Sungai Petani, Kedah, Malaysia
[f] Faculty of Medicine, Quest International University Perak, Ipoh, Perak, Malaysia

ARTICLE INFO

Keywords:
Selenium
N-Heterocyclic carbenes
NHC
Se-NHC
Breast cancer (MCF-7)
Cervical cancer (Hela)
Retinal Ganglion cancer (RGC-5)

ABSTRACT

Three benzimidazolium salts (**III-V**) and respective selenium adducts (**VI-VIII**) were designed, synthesized and characterized by various analytical techniques (FT-IR and NMR ^{1}H, ^{13}C). Selected salts and respective selenium *N*-Heterocyclic carbenes (selenium-NHC) adducts were tested *in vitro* against Cervical Cancer Cell line (Hela), Breast Adenocarcinoma cell line (MCF-7), Retinal Ganglion Cell line (RGC-5) and Mouse Melanoma Cell line (B16F10) using MTT assay and the results were compared with standard drug 5-Fluorouracil. Se-NHC compounds and azolium salts showed significant anticancer potential. Molecular docking studies of compounds (**VI, VII** and **VIII**) showed strong binding energies and ligand affinity toward following angiogenic factors: VEGF-A (vascular endothelial growth factor A), EGF (human epidermal growth factor), HIF (Hypoxia-inducible factor) and COX-1 (Cyclooxygenase-1) suggesting that the anticancer activity of adducts (**VI, VII** and **VIII**) may be due to their strong anti-angiogenic effect. In addition, compounds **III-VIII** were screened for their antibacterial and antifungal potential. Adduct **VI** was found to be potent anti-fungal agent against *A. Niger* with zone of inhibition (ZI) value 27.01 ± 0.251 mm which is better than standard drug Clotrimazole tested in parallel.

1. Introduction

Selenium containing compounds are promising candidates for cancer therapy due to their ability to alter various physiological functions involved in cancer development, presenting either anticancer, antimicrobial, antioxidant, anti-inflammatory, anti-viral, anti-neurodegenerative, anti-depressant, anti-neoplastic and chemo preventive activities [1–18]. Selenium is essential micronutrient [9,19–21] which is non-toxic to humans in low concentrations, therefore an adduct that releases selenium to the biological system in a steady rate act as an effective pharmaceutical agent [22]. The effectiveness of selenium adducts as an anti-infective agent depends on the bioavailability of selenium at the site of action [23]. Different factors such as route of delivery, ionization and solubility of adducts can affect the bioavailability of Selenium. The application of selenium containing adducts in cancer treatment and prevention is a captivating field for selenium research as they have been proven as effective anti-carcinogenic agents in different models, such as chemically induced, spontaneous and culture or transplanted tumors [24–29]. Different researchers use versatile approaches to synthesize selenium adducts. Among them, ebselen, 1,4-anhydro-5-seleno-D-talitol (SeTal), diphenyl diselenide, m-trifluoromethyl-diphenyl diselenide, 3-(4-fluorophenylselenyl)-2,5-diphenylselenophene, selenomethionine (SeMet) and bis-selenide have been recognized as promising pharmacological agents that is helpful to reduce the risk of various diseases like cancer, alzheimer, oxidative stress, HIV and depression [30–32]. Beyond these it also prevents ferroptosis which is induced by hydroperoxide [33]. Some selenium containing compounds e.g., ebselen is under the clinical trial of phase II for the treatment and prevention of noise and chemotherapy-induced hearing loss and advance stage cancers and its derivative ethaselen is under clinical trials of 1st phase [34,35]. The use of selenium in medicinal chemistry is helpful to cure many kinds of illness due to compatibility with the biological system as compared to the other already used elements of periodic table e.g., Selenium supplements are given to repay

* Corresponding authors at: Department of Chemistry, University of Agriculture, Faisalabad 38040, Pakistan (M.A. Iqbal).
E-mail addresses: adnan.iqbal@uaf.edu.pk (M.A. Iqbal), haq_nawaz@uaf.edu.pk (H.N. Bhatti).

https://doi.org/10.1016/j.bioorg.2019.103042
Received 11 February 2019; Received in revised form 22 May 2019; Accepted 3 June 2019
Available online 07 June 2019
0045-2068/

its deficiency while selenium sulphide is used in shampoos for treatment of dandruff [36,37]. Keeping in view these observations and in continuation of our previous work to synthesize new bioactive selenium *N*-heterocyclic derivatives by facile and greener methods using water as solvent (Iqbal et al., 2016b), the current study has been carried out with the hope to get better anti-cancer and anti-microbial agents.

2. Results and discussion

2.1. Synthesis and characterization

The syntheses of azolium salts (**III-V**) and respective Se-NHC adducts (**VI-VIII**) were carried out according to our previously reported work [38]. The preliminary indications for the successful synthesis of desired compounds (**III-VIII**) were the solubility, physical states, and a difference in the melting points (mp) of benzimidazolium salts and their respective selenium adducts. For example, the Se-NHC adducts were found as sticky brown material which on recrystallization gave either light yellow thick fluid which turned colorless on recrystallization compared to the benzimidazolium salts which appeared as white solids in the reaction medium depending upon the substitution of alkyl chain on nitrogen atoms of benzimidazole group. Furthermore, the selenium adducts (**VI-VIII**) were found to be soluble in non-polar solvents like chloroform, dichloromethane, *n*-hexane and diethyl ether compared to the benzimidazolium salts which are soluble in polar solvents like water, methanol and ethanol. Moreover, the difference in melting points (mp) of the benzimidazolium salts (**III-VI**) and their respective Se-NHC adducts (**VI-VIII**) provided a clear indication of successful synthesis of **VI-VIII** (Scheme 1). As the melting points of all the synthesized salts were found in the range of 110–235 °C and their respective Se-NHC adducts (**VI-VIII**) were found in 90–135 °C, which distinguish the inorganic and organic nature of synthesized compounds, respectively. The percentage yields of these compounds were found in the range of 69–85% and remain stable in the presence of moisture and air.

2.2. Spectroscopic studies

The synthesized compounds were characterized by FT-IR, ^{1}H and ^{13}C NMR. To find the spectral changes of benzimidazolium salts and their respective selenium adducts before and after the predicted bonding of elemental selenium, show some specific changes which could be used as prelude information for the successful insertion of elemental selenium, to the organic framework. In our previous work on Se-NHC adducts [39–41], we have reported that after the incorporation of selenium element to carbene carbon (C = Se) bond for imidazole has a vibrational band at 1222 cm^{-1} and a distinct spectral change appears in the region 1100–1600 cm^{-1}. Some prominent peaks in azolium salts suppressed in selenium adducts and some of them enhanced (see supplementary file, Figs. S5–S7). In general, the vibrational bands due to N−C═Se and aromatic C═C disturb prominently providing a preliminary indication of successful synthesis. Same behavior was observed in our newly synthesized compounds (**III-VIII**). But our work on silver showed four finger pattern in a region between 1200 and 1500 cm^{-1} which is completely different from selenium compounds [42]. After successful preliminary indications from physical properties

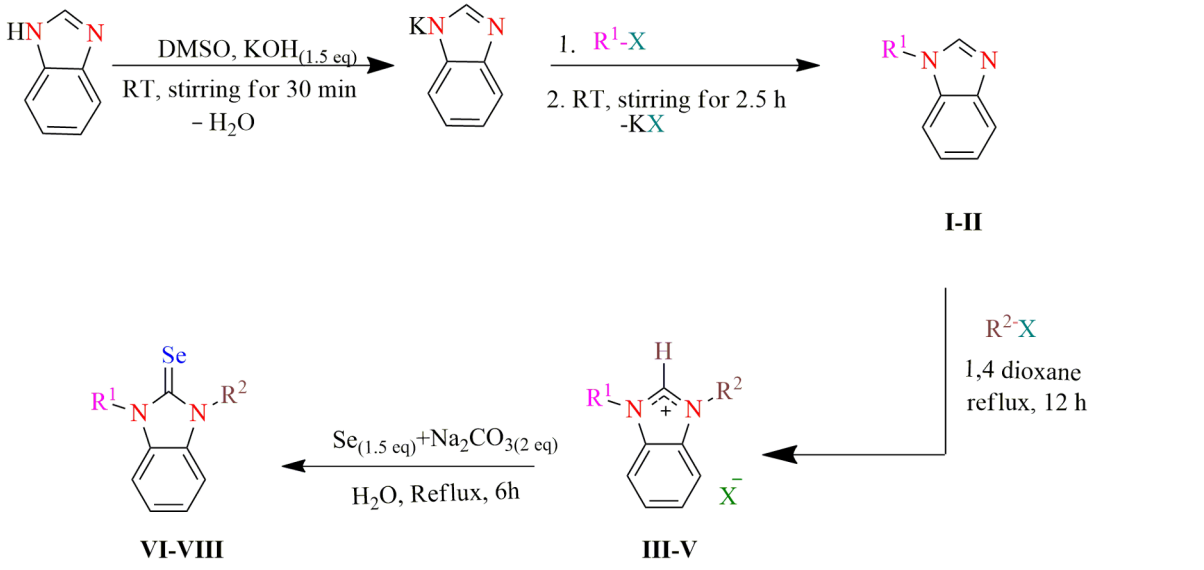

Compound	Alkyl (R) group	
	R^1	R^2
I	Benzhydryl	-
II	Octyl	-
III & VI	Benzhydryl	2-ethyl phenyl
IV & VII	Octyl	Octyl
V & VIII	Benzhydryl	Octyl

Scheme 1. General Synthesis of Benzimidazolium salts (**III-V**) and their respective selenium adducts (**VI-VIII**).

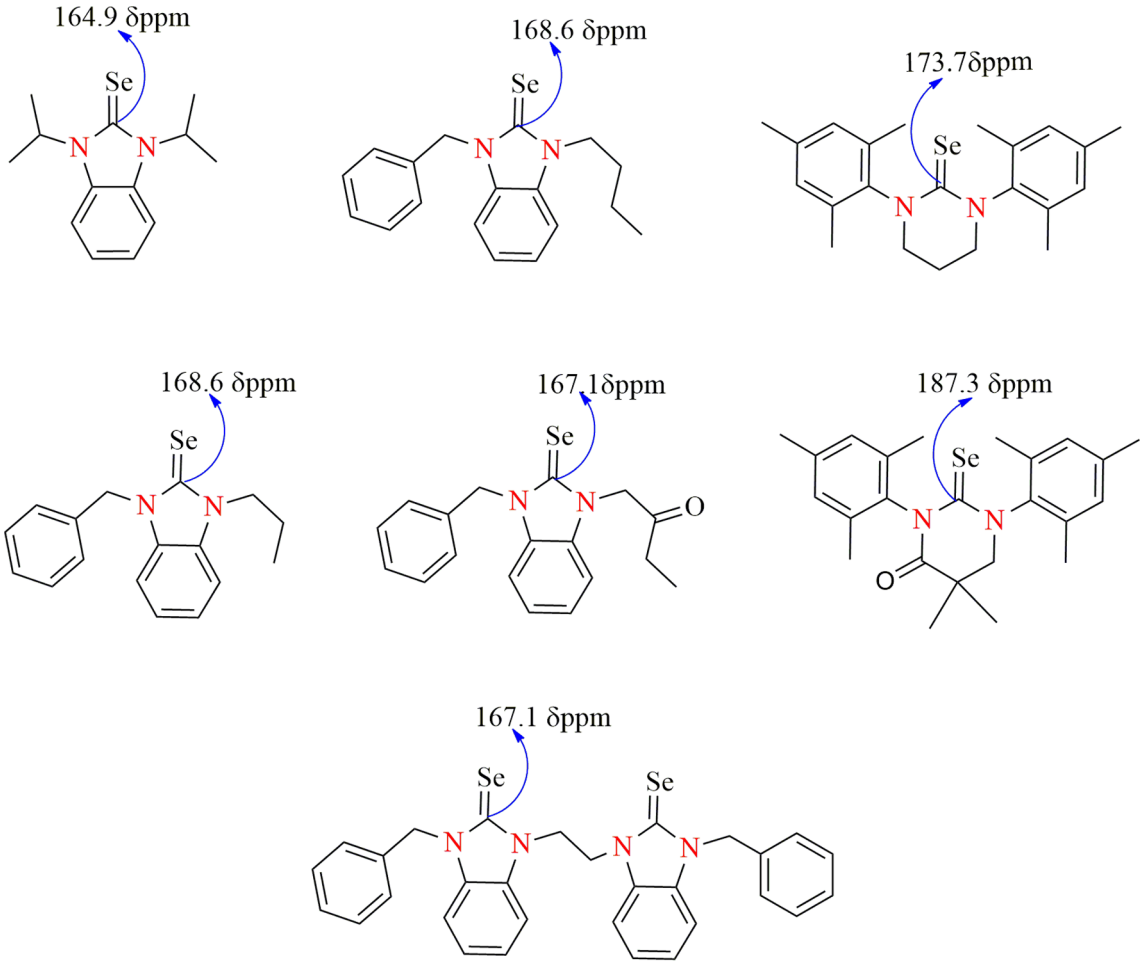

Fig. 1. Shows NMR (^{13}C) chemical shifts of Se-NHC adducts reported by other researchers highlighting variation in chemical shifts indicating the effect of ring size and substitutions on ^{13}C NMR Chemical shifts.

and FT-IR, synthesized compounds (**III-VIII**) were also confirmed by ^{1}H and ^{13}C NMR. ^{1}H NMR spectra of benzimidazolium salts **(III-V)** have a distinctive proton signal due to NCHN at 9.81–10.1 δ ppm. However, this peak (NCHN) disappeared in Se-NHC compounds **VI-VIII** due to replacement of proton with selenium. This result further verified the successful synthesis of Se–NHC adducts. ^{13}C NMR spectra of salts **(III-V)** indicated that the NCN carbon remained in up field region (142–148 δ ppm) in azolium salts as compared to selenium adducts **(V-VIII)** which appeared in the range ~165–168 δ ppm which is according to the previous reports [34,43–45] and is another significant indication (other than FT-IR) for the successful synthesis of desired compounds (see supplementary data for details Figs. S1–S7). Chemical shift of C═Se varies and becomes more versatile with the change of substitutions over imidazole/benzimidazole ring and ring size (Fig. 1) [39,44].

2.3. Antimicrobial activity

The synthesized compounds were tested against different microorganisms (bacterial and fungal strains) in addition to the cytotoxicity against targeted cancer cell lines. Thus the antimicrobial activity of the synthesized salts **(III-V)** and respective Se-NHC adducts **(VI-VIII)** were evaluated against *E. coli* (*Escherichia coli*), *B. subtilis* (*Bacillus subtilis*), *S. aureus* (*Staphylococcus aureus*) and *A. niger* (*Aspergilius Niger*) by a disc diffusion method [46]. Zones of inhibition (mm) are summarized in Fig. 3 (see supplementary file for tabulated values). In general, most of the compounds showed good to moderate activity against all tested strains. Comparing the zone of inhibition (ZI) values of synthesized compounds (**III-VIII**) with the previously published compounds (1–9, Fig. 2), it could be noticed that the selenium adduct **VIII** showed ZI value (20.01 ± 0.32 mm) better than most of the previously published selenium adducts against *E. coli.* Similarly, compounds **III, VI** & **VII** were active against *B. Subtilis*. On the other hand, compounds **III, V, VI** and **VIII** were the most active against *A. niger* (Fig. 3).

In the current study, it was also observed that some selenium adducts are active than their respective salts. However, previous reports demonstrated that selenium compounds showed poor antibacterial activity as compared to their salts. Pronounced activity of salts might be due to presence of electronegative element like chlorine and bromine. From previous experience it was noticed that presence of electronegative element is responsible for increasing antimicrobial activity [19,45,47]. The good activity of our salts may be due to same reason. In addition, selenium compounds have also shown moderate to good activity.

2.4. Anticancer studies

The synthesized salts **(III-V)** and their respective selenium adducts **(VI-VIII)** were preliminarily tested against *Cervical Cancer* Cell line (Hela), *breast adenocarcinoma (MCF-7)*, *Retinal Ganglion* Cell line (*RGC-5*) and *Mouse Melanoma* Cell line (*B16F10*) using MTT assay and compared their cytotoxicity with standard drug 5-Fluorouracil in vitro. IC_{50} values were calculated for selected compounds (Table 1**).**

Synthesized compounds demonstrated different levels of cytotoxicity against different cell lines. Percentage inhibition (% inhibition) of cell proliferation was evaluated at different concentrations of compounds (**III-VIII**) ranging from 6.125 to 100 μm [34]. From the results

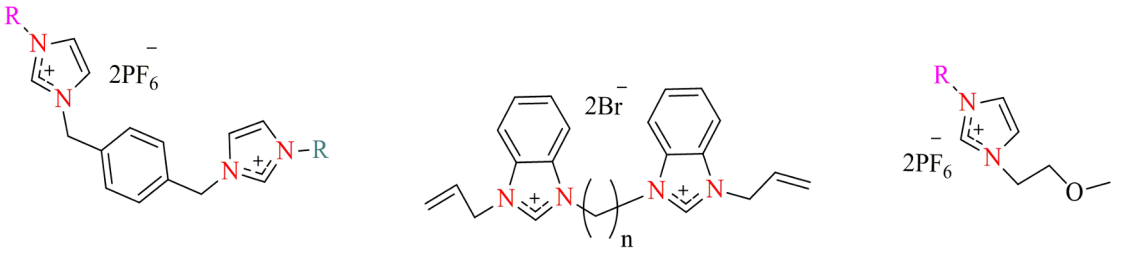

1: R=Propargyl, **2:** R= Pentyl
3:R=Methoxyethyl, **4:** R=Hexyl

5:n=2, **6:** n=3

7: R=Propyl, **8:** R= Pentyl
9: R=Butyl

Fig. 2. Chemical structures of some previously reported compounds representing different ZI value against *A. Niger, E. coli, B. subtilis* and *S.aureus* depending on the substitutions [32].

obtained through *Hela, MCF-7, RGC-5* and *B16F10* cancer cell lines, it is possible to compare the anticancer activity of salt (**III-V**) and its selenium adducts (**VII-VIII**), and to learn from factors Such as specificity, selectivity and of their cytotoxic and/or anti-proliferation effects. Fig. 4 depict the dose-dependent anticancer effects of the salts (**III-V**) and selenium adducts (**VII-VIII**) against all tested cancer cell lines. It is clearly shown in Fig. 4, as the concentration of tested sample increases, percentage inhibition of cancer cells increases. As treatment of Hela and RGC-5 cells with Salt **III** exhibited the most profound activity with IC_{50} = 0.04 ± 0.31 μM & 11.67 ± 0.18 μM, respectively. From Fig. 5, it is clearly demonstrated that the population of Hela cells reduced significantly with almost complete cell inhibition in salt **III**.

Comparison of IC_{50} values of synthesized salts and their corresponding adducts with standard drug, 5-fluorouracil (5-Fu) showed that salt **III, V** and their respective Se-NHC adducts **VI** &**VIII** showed the cytotoxic results even better than 5-Fu against *Hela* and *RGC-5* cell lines. Fig. 5 shows the selected cell images of *Hela, MCF-7, RGC-5* and *B16F10* cell lines with 48 h control without and with test drugs. It can be observed that all the cell lines have confluent growth of cancerous cells under negative control whereas under the influence of standard drug (5-Fu) a drastic decrease in cancerous cell concentration occurred indicating the death of cancer cells under standard drug tested in parallel to the test compounds. The test compound III significantly inhibited the cell proliferation comparted to the standard drug however the figure indicates different patterns of MCF-7 cell death by III compared to 5-Fu. Similar effects may be observed for cell line B16F10 and RGC-5 insisting the speculation of cell death under different mechanisms of action by test compounds and standard drug in the selected cell lines. However, the conditions are different for HeLa cell line where the cell death by standard drug and test compounds III and VI seems identical indicating the similar mechanism of action. However, such observations are merely speculations without detailed mechanistic assays.

2.5. Molecular docking

Angiogenesis is necessary for metastasis and growth of cancer cells. It is initiated by imbalance between negative and positive angiogenic factors produced by both cancer and normal cells. A currently successful strategy for the cancer treatment is targeting angiogenesis by suppressing angiogenic factors. In most of the cancers, the level of VEGF-A (vascular endothelial growth factor A), EGF (human epidermal growth factor), HIF (Hypoxia-inducible factor) and COX-1 (Cyclooxygenase-1) have been correlated with metastasis and tumorigenesis [48–52]. Automated docking systems and specific active site of target were used to explore the binding affinity and ligand efficiency of organoselenium adducts (**VI-VIII**) on VEGF-A, EGF, COX-1 and HIF. The activity of adducts was compared with that of the standard reference (5-Fluorouracil and sunitinib). The docked conformation of VEGF-A, EGF, COX-1 and HIF with active conformation of each compounds **VI, VII, VIII, sunitinib** and **5-FU** (See Fig. 6 for chemical formula) clearly revealed that numerous potential interactions were

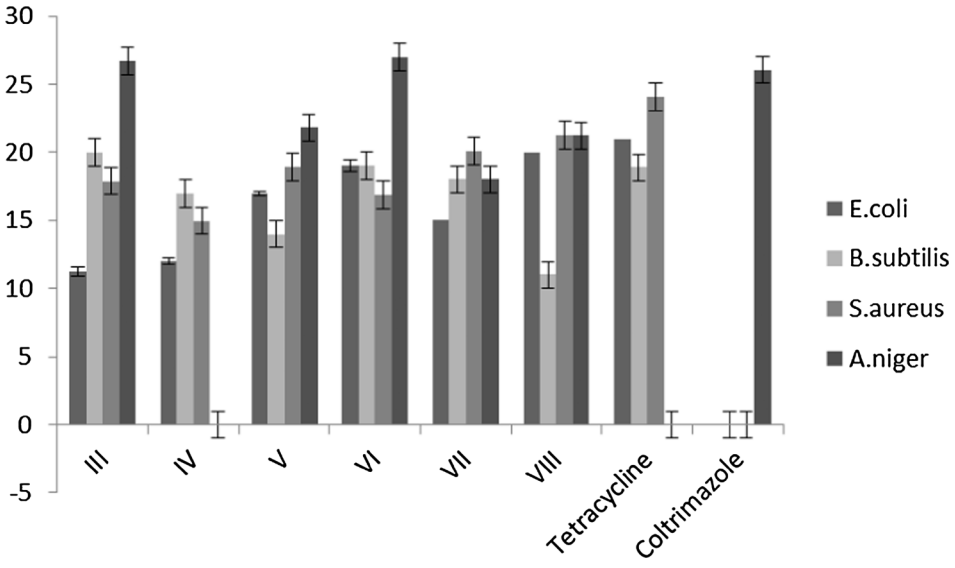

Fig. 3. *In vitro* antimicrobial activity of synthesized compounds against different pathological strains using disc diffusion method.

Table 1
IC_{50} value of tested compound against different cell lines.

	Compounds	MCF-7 (μM)	Hela (μM)	RGC-5 (μM)	B16F10 (μM)
Benzimidazolium salts	**III**	47.67 ± 0.21	0.04 ± 0.31	11.67 ± 0.18	32.22 ± 0.30
	V	8.39 ± 0.18	0.24 ± 0.22	11.63 ± 0.34	68.86 ± 0.14
Se-NHC adducts	**VI**	NT	0.11 ± 0.20	09.16 ± 0.27	386.21 ± 0.21
	VIII	66.60 ± 0.01	4.30 ± 0.11	11.61 ± 0.15	62.9 ± 0.26
Standard drug	5-Fu	11 ± 0.09	4.9 ± 0.10	16.5 ± 0.12	0.87 ± 0.15

*NT = Not tested.

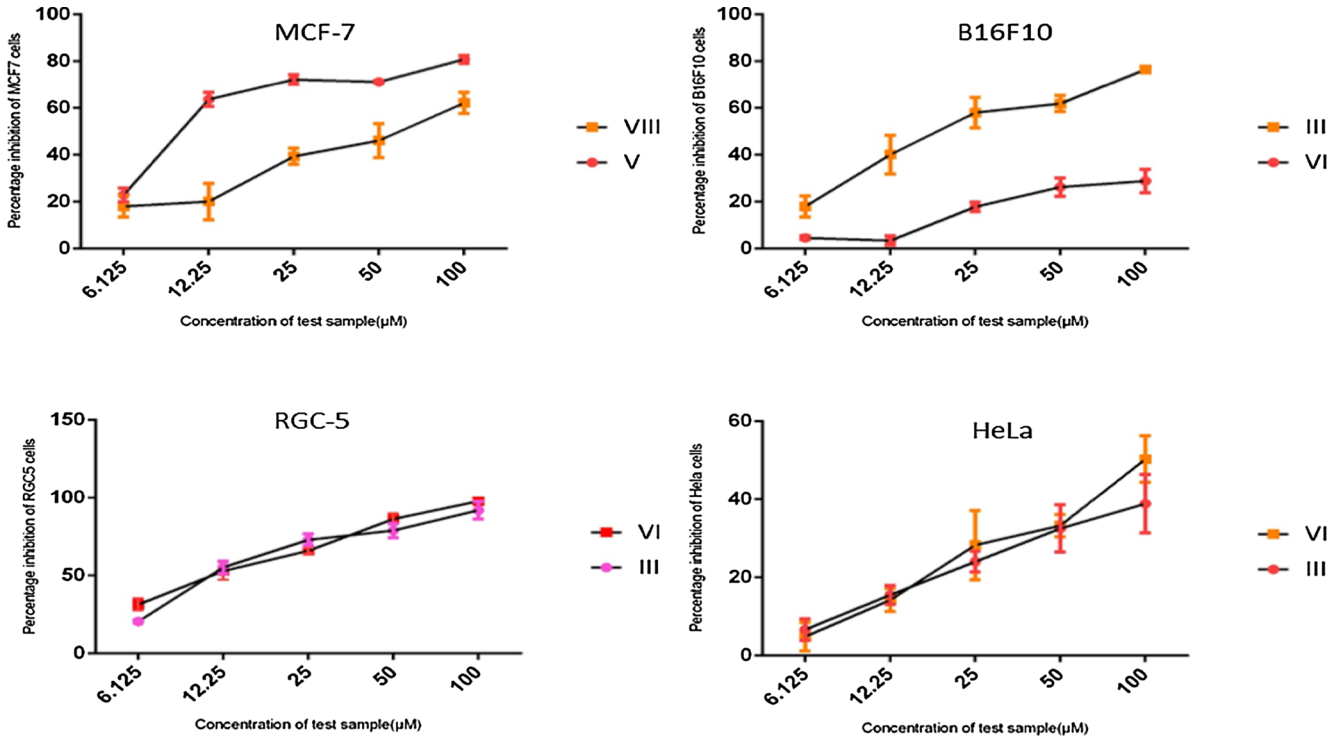

Fig. 4. Dose dependent effects of ascending amounts of selected salts and selenium adducts vs Hela, MCF-7, *RGC-5* and *B16F10* cancer cell lines on the percentage inhibition of cell proliferation.

present (Figs. 7–10). Free binding energies of **VI, VII** and **VIII** are lower than sunitinib (Table 2) which have been selected as positive control. However, compound **VII** showed higher free binding energy than 5-FU (Fig. 7). Sutent because of having two conventional hydrogen bind by GLU38 and ASP41 with VEGF, has shown strongest affinity to this target among all the tested samples.

Even though, compound **VI** because of containing four aromatic groups involved in interaction with VEGF but its affinity was still less than sutent. This was probably because of the halogen bond occurring between sutent and VEGF via SER95 strengthens best conformation between seren 50 and ASP34 this substrate and target molecule [53].

5-FU contained four hydrogens that bind with VEGFA via PHE47, PHE36, and ASP34 that made it to cause stronger affinity towards VEGFA than compound **VII**. However due to presence of one aromatic group in compound **VII**, it showed similar affinity to the target molecule as 5-FU with VEGFA. Compound **VI** and **VII** showed almost same affinity towards VEGFA as sutent even though they do not contain any conventional hydrogen bond in interaction active pocket but because of containing four and three aromatic compounds in interaction with VEGFA could stabilize it and cause lower affinity than compound **VII** and 5-FU [54]. However, compound **VI** contains Pi-sufur bond involved in binding with VEGFA protein by CYS104 and CYS26. This causes the binding pocket to be stabilized more than compounds **VI-VII** and 5-FU [54]. The free binding energy of compounds **VI**, **VII** and **VII** are lower than 5-FU which has been selected as positive control (Fig. 8). Although 5-FU involves seven conventional hydrogen binds through LEU8, CYS14, ASP11, PRO7, GLY12, TYR13 and CYS14 but compounds **VI, VII** and **VIII** can be involved in Pi-binding and contain four, one and three aromatic groups involve in Pi binding respectively which can stabilize the active pocket and cause lower binding energy in it compare to the positive control [54].

Compound **VI** contains Pi-anion binding through ASP11 and ASP17 with EGF protein (Fig. 8). This causes the binding pocket to be stabilized more than 5FU. It revealed that because it involved in pi-sulfur binding with CYS20 and CYS6 residues of EGF and stabilized and the free binding energy is less than 5FU, **VII** and **VIII**. Moreover, sutent in interaction with EGF could have only four conventional hydrogen bonds but because of stabilizing the binding HIF and 5-Fluorouracil surface pocket with Pi-Lone pair, Pi-anion and Pi sigma with EGF demonstrated less free binding energy than all other tested samples [55].

Free binding energy of compound **VI** is lower than **VII, VIII,** 5-FU and sutent with COX1. Even though sutent has made four conventional hydrogen bonds with CYS47, GLN461, GLU465 and GLN44 of COX1 but compound **VI** showed more affinity to interact with COX1 than all other tested samples. This is due to stabilization of CYS36 in COX1 that made such interactions stronger than all (Fig. 9). Although, Compounds **VII** and **VIII** also don not contain hydrogen binding in interaction with COX1 but because of containing one and three aromatic groups,

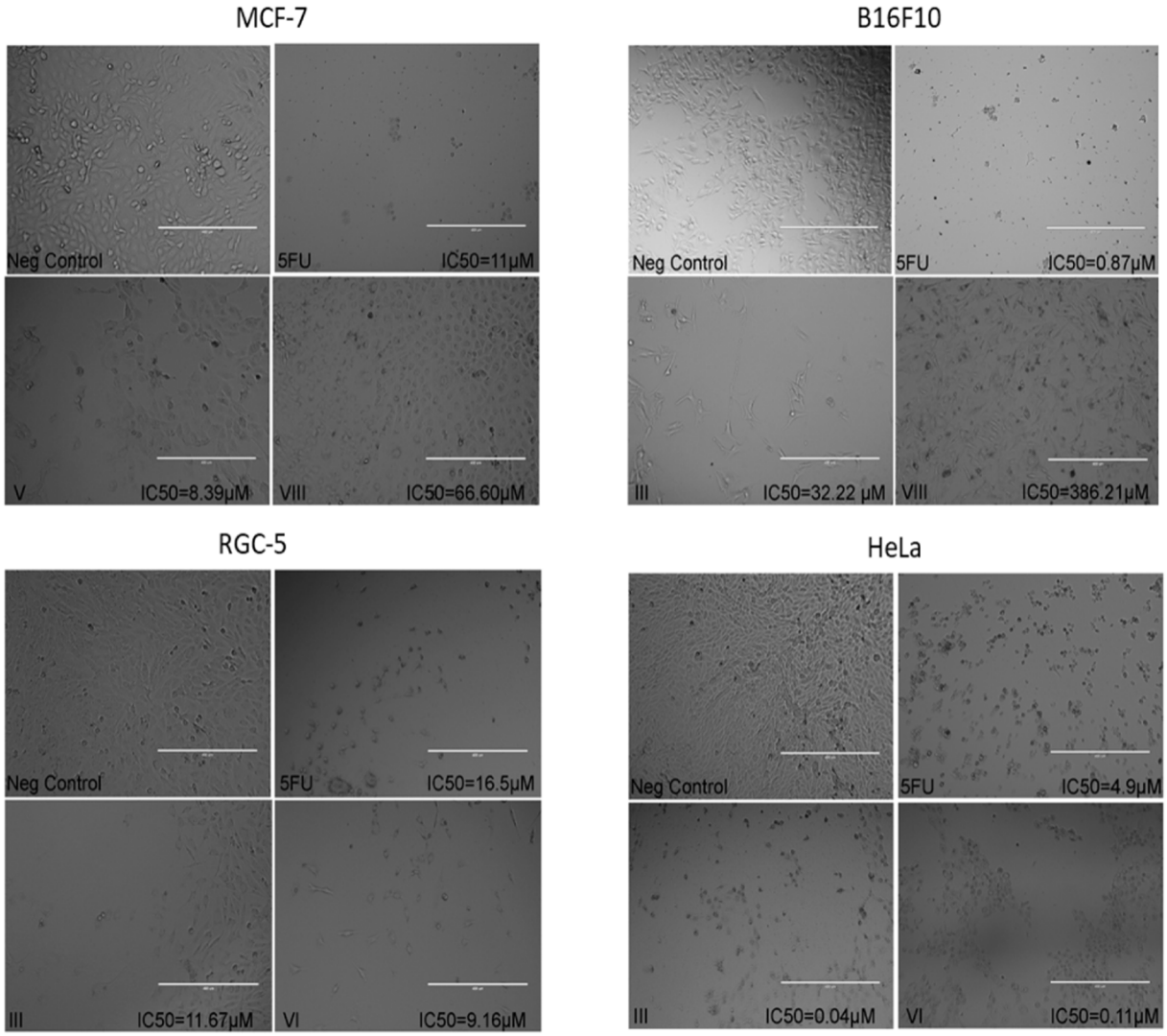

Fig. 5. MCF-7, *B16F10, RGC-5* and Hela cell images were taken with a digital camera under an inverted phase contrast microscope at * 200 magnification at 48 h after treatment with the standard drug (5-Fu) and samples.

respectively showed higher affinity than sutent and 5-FU (Fig. 9). 5-FU binds to LEU101, SER118 and GLN147 residues of HIF through conventional hydrogen bonds. Compound **VI** has shown pi-sigma interaction with VAL336 and LEU340 and because of containing four aromatic groups in its active pocket, **VI** was the strongest sample from the point of affinity towards HIF. However, compound **VIII** because of containing three aromatic groups in interaction pocket was stabilized and caused to have less free binding energy than 5-FU.

None of the studied samples in interaction with HIF were as strong as sutent because not only it could make hydrogen bond with THR39, PHE37, ARG215, ALA10 and SER11 but also obtained halogen bond with ARG33. This made very stable conformation of sutent in interaction with HIF and caused it to have the highest affinity towards this target (Fig. 10)

3. Experimental

3.1. Chemicals and instruments

All chemicals were purchased from Merck and Sigma Aldrich Chemicals and were used as such without further purifications. The melting points of adducts were determined by Stuart Melting Point SMP11. FT-IR (Fourier transform Infrared) spectra were recorded using Perkin-Elmer 2000 spectrophotometer. NMR (Nuclear magnetic resonance) spectra were collected using Bruker Avance 500. Cell culture reagents were bought from Gibco, USA; Eagle Medium, RPMI 1640 medium; Trypsin, Dulbecco's modified, and HIFBS (heat inactivated foetal bovine serum) were purchased from GIBCO, UK. *Cervical Cancer* Cell line (Hela), *breast adenocarcinom* (MCF-7), *Retinal Ganglion* Cell line (RGC-5) and *Mouse Melanoma* Cell line (B16F10) were purchased from ATCC, USA. MTT was purchased from Sigma Aldrich, Germany. DMSO (Dimethyl sulfoxide) was purchased from Fluka, USA. Stock solution (10 mM) was prepared by dissolving synthesized compounds in DMSO and stored at 4 °C. In each experiment different concentrations of solutions for different culture medium were made.

3.2. Synthesis of 1-benzhydryl-3, 2-ethyl benzene benzimidazolium bromide (III)

N-benzhydryl benzimidazole **(I)** (1.0 g, 3.52 mM) was dissolved in 1,4-dioxane (40 mL) on heating and 2-bromo ethyl benzene (0.478 mL, 3.51 mM) was then added and reflux the reaction mixture at 100 °C with consistent stirring, After 24 hr the reaction mixture was cooled to room temperature slowly and the precipitates were filtered, washed with distilled water. Yield: 1.34 g (81%). M.P.: 233–235 °C FT-IR (KBr, ν cm^{-1}): 3210, 3120, 3011 (C-H_{arom} stretch), 2974, 2879 (C-H_{aliph}

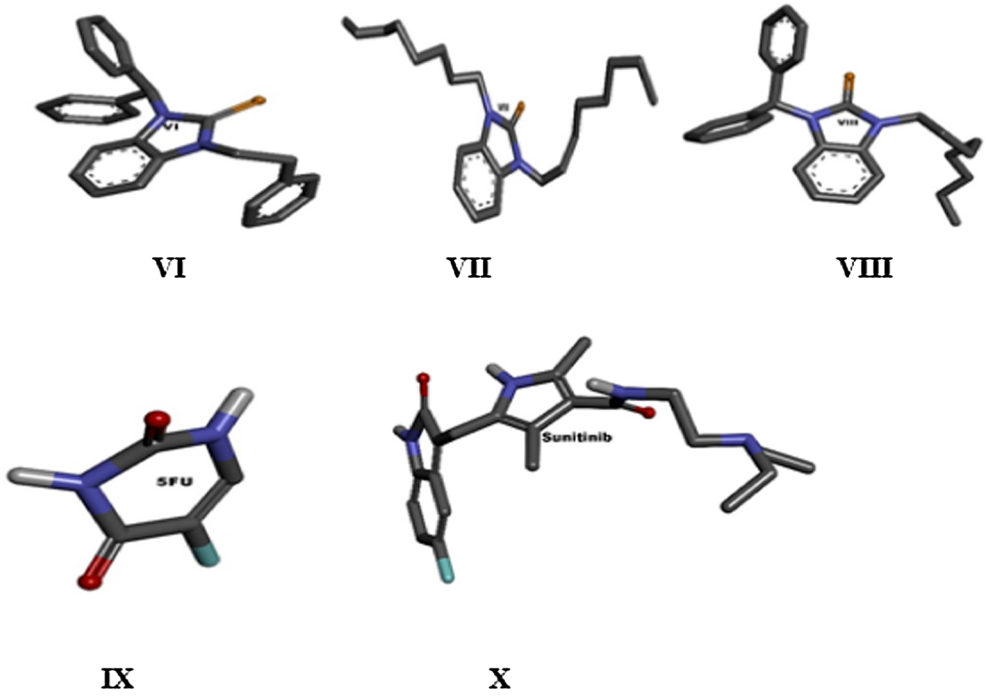

Fig. 6. 2D view of VI, VII, VIII, IX (5-Fu) and X (sunitinib).

stretch), 1660, 1598 (C = C_{arom} stretch), 1476, 1336, 1314 (CH_2 bendings). ^{1}H NMR (300 MHz, DMSO-d_6, δppm): 3.25(t, 2H, 1 × CH_2, J = 6 Hz), 4.85 (t, 2H, 1 × CH_2, J = 9 Hz), 5.70 (s, 1H, CH–), 6.94 (q, 1H, Ar-H), 7.21 (m, 10*H*, Ar-H), 7.31 (m, 4H, Ar-H, d), 7.80 (d, 2H, J = 30 Hz Ar-H), 9.18 (s, 1H, NCHN). ^{13}C NMR (125.1 MHz, DMSO-d_6, δppm): 34.7 (*C*H_3), 62.5 (*C*H_2), 64.3 (N-*C*H_2), 74.7, (Ar-*C*H-N), 114.7, 114.8, 120.1, 122.1, 123.7, 127.4, 128.2, 129.1, 129.7, 131.4, 136.3, 137.1, 139.1, 142, 148 (N*C*HN). Anal. Calcd for $C_{28}H_{25}BrN_2$: C, 71.64; H, 5.37; N, 5.97; Found: C, 71.52; H, 5.47; N, 5.83.

3.3. Synthesis of 1,3-dioctyl-benzimidazolium bromide (IV)

N-octyl benzimidazole (**II**) (1 g, 4.34 mM) was dissolved in 1, 4-dioxane (20 mL) and *n*-octyl bromide (1.62 g, 1.46 mL) was then added. The reaction mixture was refluxed for 24 hr continuously. Shiny white crystals were obtained within few hours. Yield: 1.2 g (83%). M.P: 111–113 °C. FT-IR (KBr, ν cm^{-1}): 3475, 3401, (C-Harom stretch), 2971, 2936, 2875 (C-H_{aliph} stretch), 1615, 1557, 1458 (C = Carom stretch), 1377 (CH_2 bending). ^{1}H NMR (500 MHz, DMSO-d_6, δ ppm): 0.80 (6H, t, 2 × CH_3, J = 7.1 Hz), 1.24 (20H, m, 10 × CH_2), 1.90 (4H, t, , 2 × CH_2, J = 6.94 Hz), 4.51(4H, t, Ar-CH_2-N, J = 7.7 Hz), 7.68(2H, m, Ar-H), 8.10 (2H, m, Ar-H), 10.1 (1H, s, NCHN). ^{13}C NMR (125.1 MHz, DMSO-d_6, δ ppm): 14.3 (CH_3), 22.5, 26.2, 28.8, 31.6 (R-CH_2), 47.2 (N-CH_2-R), 114.2, 126.9, 131.5, (Ar-C), 142.5 (NCHN). Anal. Calcd for $C_{23}H_{39}BrN_2$: C, 65.23; H, 9.28; N, 6.62; Found: C, 65.15; H, 9.39; N, 6.72.

3.4. Synthesis of 1-benzhydryl-3-octyl benzimidazolium bromide (V)

N-benzhydryl benzimidazole **(I)** (0.51 g, 1.76 mM) was dissolved in 1, 4-dioxane (20 mL) and *n*-octyl bromide (1.62 g, 1.46 mL) was then added. The reaction mixture was heated to reflux (100 °C). A brown liquid is obtained. Solvent extraction was done using chloroform. Pass the reaction mixture from six plies of wattman filter paper. After that pass the filtrate through celite, a light brown thick liquid was obtained. Yield: 1.1 g (79%). M.P: 113–115 °C. FT-IR (KBr, ν cm-1): 3022 (C-Harom stretch), 2972, 2936, (C-Haliph stretch), 1498, 1458 (C = Carom stretch), 1377 (CH_2 bending). ^{1}H NMR (500 MHz, DMSO-d_6, δ ppm): 0.82 (3H, t, CH_3, J = 7.16 Hz), 1.22 (10*H*, m, 10), 1.89 (2H, t, CH_2, J = 7.45 Hz), 4.56(2H, t, Ar-CH_2-N, J = 7.43 Hz), 7.45(10*H*, m, Ar-H), 7.6 (1H, t, CH_2, J = 7.53 Hz), 7.69 (2H, m, Ar-H), 7.7 (1H, d, Ar-H, J = 8.45 Hz), 8.2 (1H, d, Ar-H, J = 8.7 Hz) ,9.6 (1H, s, NCHN), 21.6 (CH_2), 48.1 (N-CH_2), 50.1 (Ar-CH-N), 113.7, 127.2, 128.2, 129.9, 130.1, 131.7, 134.9 (Ar-C), 142.2 (NCHN). ^{13}C NMR (125.1 MHz, DMSO-d_6, δ ppm): 14.4 (CH_3), 22.5, 26.2, 28.8, 39.1, 31.5 (R-CH_2), 47.5, 64.4 (N-CH_2-R), 114.6, 114.9, 127.2, 128.8, 129.7, 131.6, 131.9, 136.6 (Ar-C), 142.2 (NCHN). Anal. Calcd for $C_{28}H_{33}BrN_2$: C, 70.43; H, 6.97; N, 5.87; Found: C, 70.27; H, 7.13; N, 5.97.

3.5. Synthesis of 1-benzhydryl-3–2 ethyl benzene-benzimidazole-2-selenone (VI)

Salt **III** (1 g, 2.51 mM) was dissolved in deionized water (50 mL) on heating using round bottom flask (100 mL). Selenium powder (0.19 g, 2.49 mM) along with Na_2CO_3 (0.46 g, 3.32 mM) were then dissolved and the reaction mixture was heated to reflux for 5 h. Oily layer appeared above the water surface along with adhered sticky material to the magnetic stirrer and unreacted selenium metal remained remains settled at the bottom of the flask. The reaction mixture was filtered through celite, washed with distilled water (3 × 5 mL) and was extracted using chloroform. A White powder was obtained which on recrystallization gives white shiny needle like crystals. Yield: 0.33 g (78%). M.P.: 133–135 °C. FT-R (KBr, ν cm^{-1}): 3294, 3060, 3027 (C-H_{arom} stretch), 2927, 2857 (C-H_{aliph} stretch), 1601, 1582, 1482 (C = Carom stretch), 1453, 1401, 1339, 1358 (CH_2 bending). ^{1}H NMR (500 MHz, $CDCl_3$, δ ppm): 3.14 (2H, t, 1 × CH_2), 4.65–4.68 (2H, t, 1 × CH_2, J = 9 Hz), 7.29–7.33 (19H, m, Ar-C) 8.14(1H, s) ^{13}C NMR (125.1 MHz, $CDCl_3$, δ ppm): 34.3 (R-CH_2), 57.1(N-CH_2-R), 72.0 (Ar-*C*H-N), 118.6, 125.9, 126.2, 128.2, (Ar-*C*), 130.5(R-CH-N), 139.4(R-CH-R), 142.7(Ar-CH), 167.8 (*C* = Se). Anal. Calcd for $C_{28}H_{24}N_2Se$: C, 71.94; H, 5.17; N, 5.99; Found: C, 71.81; H, 5.25; N, 5.79.

3.6. Synthesis of 1,3-dioctyl-benzimidazole-2-selenone (VII)

Salt **III** (1 g, 2.09 mM) was dissolved in 50 mL distilled water on heating using 100 mL two neck round bottom flask. Selenium metal

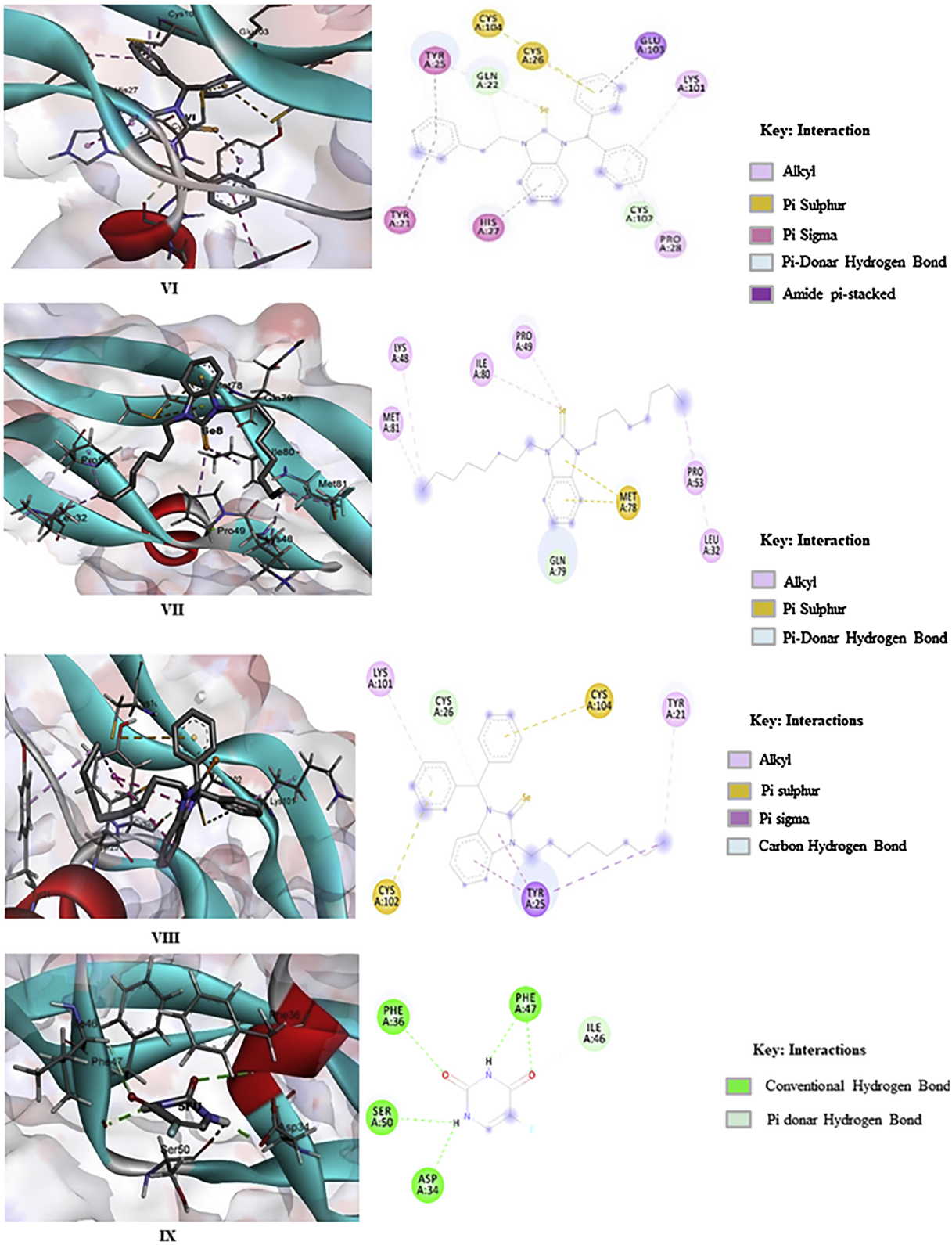

Fig. 7. Visualization of ligands and protein interaction profile: **VI**: VEGF with - VI surface, **VII**: VEGF with – VII, **VIII:** VEGF with - VIII surface, **IX**: VEGF with - IX surface and their respective active site residue interaction.

powder (0.24 g, 3.04 mM) along with Na_2CO_3 (0.44 g, 4.15 mM) were then added and refluxed for 4 h. After 4 h dark brown oily layer appeared above the reaction mixture along with adhered sticky material to the magnetic stirrer and unreacted selenium metal remained settled with magnetic stirrer at the bottom of the flask. To remove unreacted selenium metal filter the reaction mixture by using celite. Extarction of oily layer was done by solvent extraction method using chloroform as solvent. Washing was done by acetonitrile (3 × 5 mL). A thich dark brown liquid was obtained. Yield: 0.78 g (82%). M.P.: 99–101 °C. FT-R (KBr, ν cm^{-1}): 2927, 2857 (C-H_{aliph} stretch), 1705, 1660, 1596, 1476

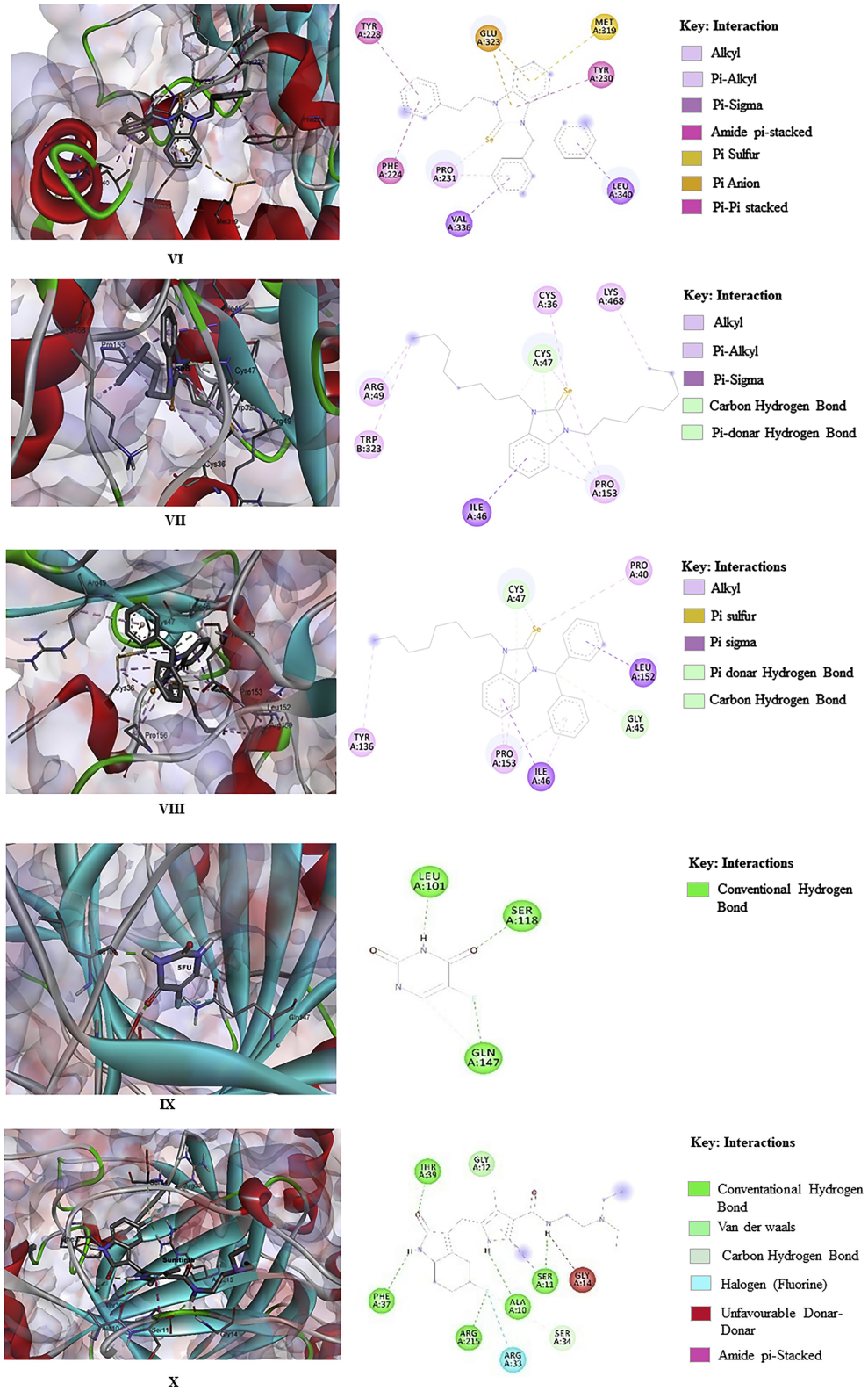

Fig. 8. Visualization of ligands and protein interaction profile: **VI**: EGF with – VI surface, **VII**: EGF with – VII, **VIII:** EGF with – VIII surface, **IX**: EGF with – IX surface, **X**: EGF with – X surface and their respective active site residue interaction.

(C = Carom stretch), 1492, 1448, 1406, 1392 (CH_2 bending) ^{1}H NMR (500 MHz, $CDCl_3$, δ ppm): 0.86(6H,t, J = 6.8 Hz), 1.20(20H, m, 10 × CH_2), 1.71(2H, t, CH_2, J = 7.16 Hz), 1.85(2H, t, CH_2, J = 7.52 Hz) 4.40 (2H, t, N-CH_2, J = 7.70 Hz), 6.90(2H, m, Ar-H), 7.07(2H, m, Ar-H), 7.21(2H, m, Ar-H). ^{13}C NMR (125.1 MHz, $CDCl_3$, δ ppm): 13.6 (CH_3), 22.2, 26.4, 28.7, 31.3(R-CH_2), 46.2, 47.2 (Ar-*C*H-N), 112.6, 120.4, 122.6, 129, (Ar-*C*), 165.01 (*C* = Se). Anal. Calcd for $C_{23}H_{38}N_2Se$: C, 65.54; H, 9.09; N, 6.65; Found: C, 65.63; H, 9.18; N, 6.71.

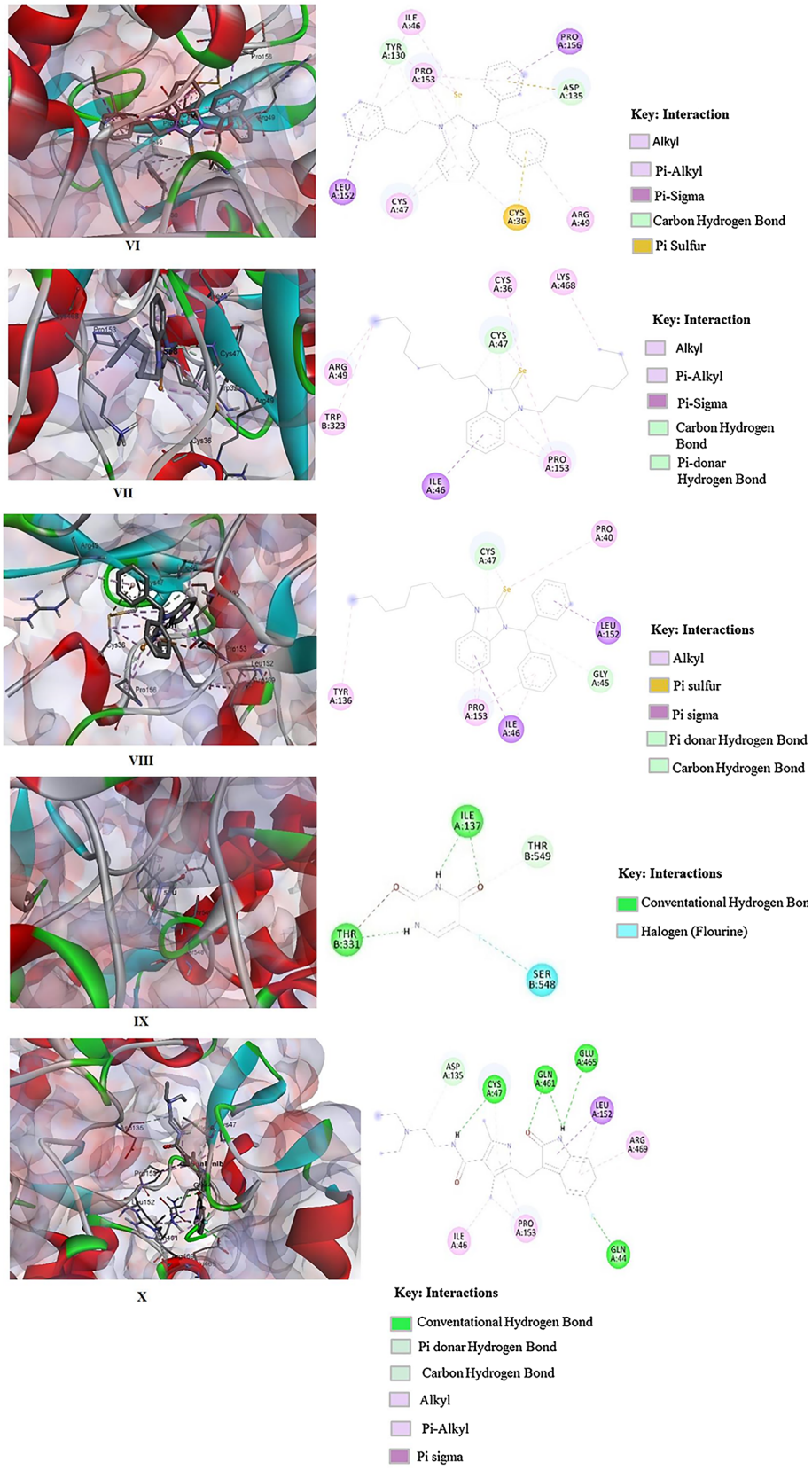

Fig. 9. Visualization of ligands and protein interaction profile: **VI**: COX1 with - VI surface, **VII**: COX1 with – VII, **VIII:** COX1 with - VIII surface, **IX**: COX1 with - IX surface, **X**: COX1 with – X surface and their respective active site residue.

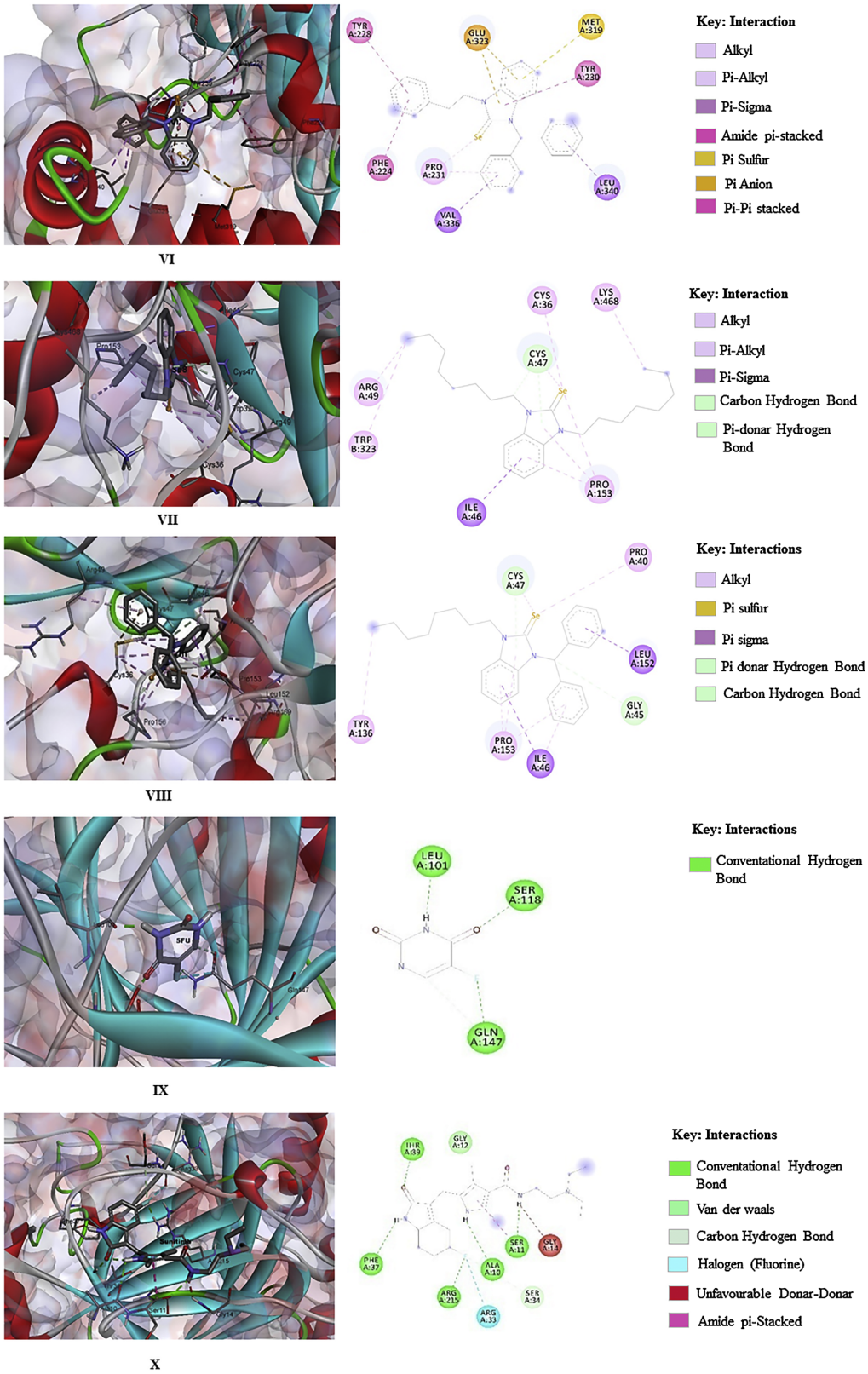

Fig. 10. Visualization of ligands and protein interaction profile: **VI**: HIF with - VI surface, **VII**: HIF with – VII, **VIII:** HIF with - VIII surface, **IX**: HIF with - IX surface, **X**: HIF with – X surface and their respective active site residue interaction.

3.7. Synthesis of 1-benzhydryl-3-octyl-benzimidazole-2-selenone (VIII)

II (0.55 g, 1.66 mM) was dissolved in distilled water (20 mL) on heat using round bottom flask (100 mL). Selenium powder (0.2 g, 2.49 mM) along with Na_2CO_3 (0.46 g, 3.32 mM) were then added and the reaction medium was heated to reflux for 5 h. Oily layer formed above the water surface along with sticky black solid attached to the magnetic stirrer and the unreacted selenium powder remained settled at the bottom of

Table 2
Binding energy and inhibition constant of compounds **VI-VIII.**

Binding energy (kJ mole^{-1})	VI	−10.53	−6.79	−6.32	−7.09
	VII.	−8.55	−4.64	−4.05	−6.46
	VIII	−9.24	−6.36	−5.25	−8.21
Standard drugs	5-Fluorouracil	−10.3	−8.11	−4.97	−8.21
	Sunitinib	−5.09	−4.97	−6.71	−5.97
Inhibition constant (μM)	VI	19.09 * 10^3	5.84	4.15	1.50
	VII	543.61 * 10^3	220.01	391.83	25.16
	VIII	76.84 * 10^3	21.93	64.11	4.08
Standard drugs	5-Fluorouracil	28.04	1.14	229.15	964.34
	Sunitinib	187.11 * 10^3	227.34	12.12	138.96 * 10^3

the flask. The reaction mixture was filtered, washed with distilled water (3 × 5 mL) and was extracted using dichloromethane. A thick brown liquid is obtained. Yield: 0.61 g (69%). M.P.: 96–98 °C. FT-IR (KBr, ν cm-1): 3084, 3055, 3027 (C-Harom stretch), 1482 (C = Carom stretch), 1453, 1405, 1337, 1358 (CH_2 bending). ^{1}H NMR (500 MHz, CDCl3, δ ppm): 0.82(3H,t, J = 7.2 Hz), 1.27(10H, m, CH_2), 1.74(2H, m, CH_2),) 4.34 (2H, m), 6.7–8.47(14H, m, Ar-H) ^{13}C NMR (125.1 MHz, $CDCl_3$, δ ppm): 14.3 (CH_3), 22.5, 26.6, 29, 31.6(R-CH_2), 46.1(R-CH_2-N) 64.9 (Ar-*C*H-N), 110.9, 112.4, 126.7, 128.4, 128.5, 129.1,137.5, 146.2 (Ar-*C*), 167.8 (*C* = Se). Anal. Calcd for $C_{28}H_{32}N_2Se$: C, 70.72; H, 6.78; N, 5.89; Se, 16.60; Found: C, 70.89; H, 6.69; N, 5.98.

3.8. In vitro antimicrobial activity

Agar disc diffusion method was used to evaluate the synthesized compounds (**III-VIII**) individually against gram positive (Staphylococcus aureus & Bacillus subtilis) and gram negative (Escherichia coli) bacterial strains as well as fungal strain A. Niger (Aspergillus Niger). In this method 100 μL of suspension containing 10^6 CFU/mL and 10^4 spores/mL of tested bacteria and fungi spread on NA (nutrient agar), and PDA (potato dextrose agar) medium respectively. Media was allowed to cool and solidified. After solidification paper discs of 6 mm diameter soaked with 80 μL of the test compounds to the agar plates and incubated at 30 °C. After one day, zone of inhibition (ZI) was measured against all the tested micro-organisms and compared with that of the standard (ampicillin and Clotrimazole).

3.9. In vitro Anti-cancer effect of synthesized compounds

The cytotoxicity effect of the compounds (**III-VIII**) was evaluated using MTT assay. micro-titer plate reader was used to read the assay plates. 5-fluorouracil (5-Fu) was used as reference (standard).

3.10. Preparation of cell culture

Initially, Hela, MCF-7, RGC-5 and B16F10 cells were grown under maximum incubated conditions. Only those cells were selected for cell plating that had reached a confluency of 75–80% Discard the old medium from plate and cells were washed twice or thrice with 7.4 pH of PBS (phosphate-buffer saline), after washing PBS was completely discarded. Now, trypsin was added and evenly distributed on the cell surfaces. Cells were incubated for 1 min at 37 °C in 5% CO_2. Then, the flasks containing the cells were gently tapped to help cell segregation and observed under inverted microscopeAfter that, trypsins were added and cells were incubated at 37 °C in 5% CO_2 for 1 min. Then, the cell segregation was observed using inverted microscope. 5 mL of fresh media (10% Fetal Bovine Serum) was added to observe trypsin activity. Finally, Added 100 mL cells per well with concentration of $2.5*10^5$ cells per mL and incubated with 5% CO_2 as internal atmosphere at 37 °C

3.11. MTT assay

MTT assay was performed according to previously reported method of our research group [38].

Molecular Docking study of Compounds VI-VIII

3.12. Protein preparation

3.12.1. Software

Python language was downloaded from www.python.com, Molecular graphics laboratory(MGL) tools was downloaded from http://mgltools.scripps.edu and AutoDock4.2 was downloaded from http://autodock.scripps.edu, Bio Via draw was downloaded from http://accelrys.com, Discovery studio visualizer 2017 downloaded from http://accelrys.com and Chem3D was downloaded from https://acms.ucsd.edu.

3.12.2. Methods

The three dimensional X-ray crystallographic structures of anticancer targets VEGF-A with PDB ID: 4KZN, COX1 with PDB ID: 1EQH, EGF with PDB ID: 1JL9, HIF with PDB ID: 1YCI were selected and downloaded from Protein Data Bank (www.rvcsb.org/pdb) (Fig. 11) [56]. To make the selected proteins for molecular docking, all non-essential water molecules, small molecules, heteroatoms, nonpolar hydrogens, nonstandard residues and lone pairs were deleted and hydrogens were added to the target receptor molecule. Optimization of geometry and minimum energy of all structures were performed using Dock Prep, a built-in tool for structures preparation before docking.

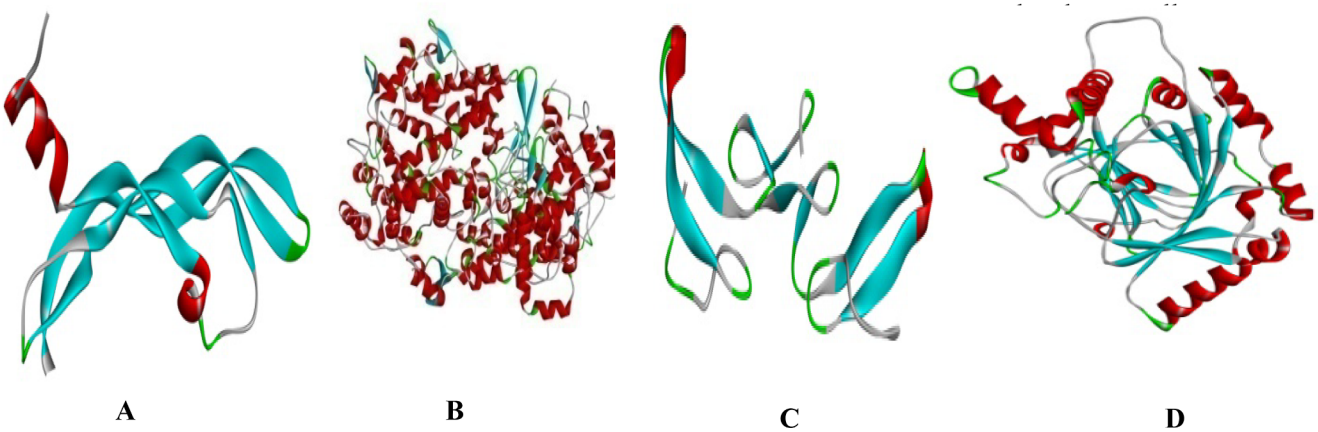

Fig. 11. A: VEGFA protein from RCSB protein data bank (4KZN), B: COX1 protein from RCSB protein data bank (1EQH), C: EGF protein from RCSB protein data bank (1JL9), D: HIF protein from RCSB protein data bank (1YCI).

3.12.3. Ligand preparation

Four synthetic active compounds available with identified structure of salts from crystallography were used Pubchem to make sdf format and converted to PDB format using Pymol and further used for docking studies towards three different cancer cells and EA.hy 926 cell line as normal cell line. The starting structures of the proteins were prepared using AutoDock tools. Water molecule was deleted, polar hydrogen and Kollman charges were added to the protein starting structure. Grid box was set with the size of 126 × 126 × 126 Å with the grid spacing of 0.375 Å at the binding site. The starting structure for all the salts namely **VI, VII** and **VIII** were constructed using BioVia draw While Sunitinib and 5FU were selected as positive control. Their structures were provided from Pubchem website Gasteiger charges were assigned into optimized ligand using Autodock tools. 100 docking runs were conducted with mutation rate of 0.02 and crossover rate of 0.8. The population size was set to use 250 randomly placed individual. Lamarckian Genetic algorithm was used as the searching algorithm with a translational step of 0.2 Å, a quaternion step of 5 Å and a torsion step of 5 Å. Most populated and lowest binding free energy

4. Conclusion

Three novel benzimidazolium salts and their respective selenium-NHC adducts were designed, synthesized and tested *in vitro* against a panel of non-fastidious fungus, bacteria and various cancerous cell lines. Adduct **VII** was particularly effective against *B. subtilis* and *A. Niger*, having the highest antimicrobial activity across the panel of microorganisms in comparison to the other adducts and their standard drugs. From MTT assay it was concluded that compounds (**III, V, VI** and **VIII)** showed better cytotoxicity than standard drug against Hela and RGC-5 while results of molecular docking study showed that, all the designed and synthesized compounds had good affinity toward the active pocket and minimum binding energy.

Declaration of Competing Interest

The authors have declared no Conflict of Interest.

Acknowledgements

Dr. Muhammad Adnan Iqbal and Prof. Haq Nawaz Bhatti are thankful to the HEC-Pakistan for the startup research grant Vide Letter No. 21-1085/SRGP/R&D/HEC/2016 to establish the organometallic and coordination chemistry laboratory at University of Agriculture, Faisalabad where a major part of this research was accomplished. Dr. MAI is also thankful to HEC-Pak for awarding research grant NRPU-8396 vide letter No. 8396/Punjab/NRPU/R&D/HEC/2017.

Appendix A. Supplementary material

Supplementary data to this article can be found online at https://doi.org/10.1016/j.bioorg.2019.103042.

References

[1] E.E. Battin, N.R. Perron, J.L. Brumaghim, The central role of metal coordination in selenium antioxidant activity, Inorg. chem. 45 (2) (2006) 499–501.
[2] M. Elsherbini, W.S. Hamama, H.H. Zoorob, Recent advances in the chemistry of selenium-containing heterocycles: five-membered ring systems, Coord. Chem. Rev. 312 (2016) 149–177.
[3] L.V. Papp, J. Lu, A. Holmgren, K.K. Khanna, From selenium to selenoproteins: synthesis, identity, and their role in human health, Antioxid. Redox Signal. 9 (7) (2007) 775–806.
[4] E.E. Battin, J.L. Brumaghim, Antioxidant activity of sulfur and selenium: a review of reactive oxygen species scavenging, glutathione peroxidase, and metal-binding antioxidant mechanisms, Cell Biochem. Biophys. 55 (1) (2009) 1–23.
[5] K. Nicolaou, J.A. Pfefferkorn, G.-Q. Cao, Selenium-based solid-phase synthesis of benzopyrans I: applications to combinatorial synthesis of natural products, Angew. Chem. Int. Ed. 39 (4) (2000) 734–739.
[6] B.F. Lirab, Synthesis and characterization of three new organo-selenium compounds. A convenient synthesis of aroylselenoglycolic acids, Arkivoc 6 (2004) 22–26.
[7] A. Kamal, M.A. Iqbal, H.N. Bhatti, Therapeutic applications of selenium-derived compounds, Rev. Inorg Chem 38 (2) (2018) 49–76.
[8] D. de Souza, D.O. Mariano, F. Nedel, E. Schultze, V.F. Campos, F. Seixas, R.S. da Silva, T.S. Munchen, V. Ilha, L. Dornelles, New organochalcogen multitarget drug: synthesis and antioxidant and antitumoral activities of chalcogenozidovudine derivatives, J. Med Chem. 58 (8) (2015) 3329–3339.
[9] M. Rother, V. Quitzke, Selenoprotein synthesis and regulation in Archaea, Biochim. Biophys Acta (BBA)-General Subjects (2018).
[10] H. Guyot, L. Alves de Oliveira, E. Ramery, J.-F. Beckers, F. Rollin, J. Trace Elemn. Med. Biol (2011).
[11] E.H. da Cruz, M.A. Silvers, G.A. Jardim, J.M. Resende, B.C. Cavalcanti, I.S. Bomfim, C. Pessoa, C.A. de Simone, G.V. Botteselle, A.L. Braga, Synthesis and antitumor activity of selenium-containing quinone-based triazoles possessing two redox centres, and their mechanistic insights, Eur. J. Med. Chem. 122 (2016) 1–16.
[12] E.E. Alberto, V.D. Nascimento, A.L. Braga, Catalytic application of selenium and tellurium compounds as glutathione peroxidase enzyme mimetics, J. Braz. Chem. Soc. 21 (11) (2010) 2032–2041.
[13] H. Elshaflu, T. Todorović, M. Nikolić, A. Lolić, A. Višnjevac, S. Hagenow, J.M. Padrón, A.T. García-Sosa, I. Djordjević, S. Grubišić, Selenazolyl-hydrazones as novel selective MAO inhibitors with antiproliferative and antioxidant activities: experimental and in-silico studies, Front. Chem. 6 (2018) 247.
[14] E.R. Tiekink, Therapeutic potential of selenium and tellurium compounds: opportunities yet unrealised, Dalton Trans. 41 (21) (2012) 6390–6395.
[15] I.L. Martins, J.P. Miranda, N.G. Oliveira, A.S. Fernandes, S. Gonçalves, A.M. Antunes, Synthesis and biological activity of 6-selenocaffeine: potential modulator of chemotherapeutic drugs in breast cancer cells, Molecules 18 (5) (2013) 5251–5264.
[16] C. Sanmartin, D. Plano, J.A. Palop, Selenium compounds and apoptotic modulation: a new perspective in cancer therapy, Mini-Rev. Med. Chem. 8 (10) (2008) 1020–1031.
[17] M. Ninomiya, D.R. Garud, M. Koketsu, Biologically significant selenium-containing heterocycles, Coord. Chem. Rev. 255 (23) (2011) 2968–2990.
[18] A.A. Vieira, I.R. Brandao, W.O. Valença, C.A. de Simone, B.C. Cavalcanti, C. Pessoa, T.R. Carneiro, A.L. Braga, E.N. da Silva, Hybrid compounds with two redox centres: modular synthesis of chalcogen-containing lapachones and studies on their antitumor activity, Eur. J. Med. Chem. 101 (2015) 254–265.
[19] E.E. Alberto, L.L. Rossato, S.H. Alves, D. Alves, A.L. Braga, Imidazolium ionic liquids containing selenium: synthesis and antimicrobial activity, Org. Biomol. Chem. 9 (4) (2011) 1001–1003.
[20] N.D. Solovyev, Importance of selenium and selenoprotein for brain function: from antioxidant protection to neuronal signalling, J. Inorg. Biochem. 153 (2015) 1–12.
[21] T. Liu, T. Yang, Z. Xu, S. Tan, T. Pan, N. Wan, S. Li, MicroRNA-193b-3p regulates hepatocyte apoptosis in selenium-deficient broilers by targeting MAML1, J. Inorg. Biochem. 186 (2018) 235–245.
[22] P. Du, U.M. Viswanathan, Z. Xu, H. Ebrahimnejad, B. Hanf, T. Burkholz, M. Schneider, I. Bernhardt, G. Kirsch, C. Jacob, Synthesis of amphiphilic seleninic acid derivatives with considerable activity against cellular membranes and certain pathogenic microbes, J. Hazard. Mater. 269 (2014) 74–82.
[23] M. Abbady, M. Kandeel, S.H. Abdel-Hafez, M.-A. Abou-Omar, Organic selenium compounds, Part IV: Synthesis and applications of some new diaryl selenides containing azomethine and oxazole moieties, Phosphorus, Sulfur Silicon 185 (8) (2010) 1708–1725.
[24] L. Zhao, J. Li, Y. Li, J. Liu, T. Wirth, Z. Li, Selenium-containing naphthalimides as anticancer agents: design, synthesis and bioactivity, Bioorg. Med. Chem. 20 (8) (2012) 2558–2563.
[25] B. Banerjee, M. Koketsu, Recent developments in the synthesis of biologically relevant selenium-containing scaffolds, Coord. Chem. Rev. 339 (2017) 104–127.
[26] V. Dotsenko, K. Frolov, S. Krivokolysko, Chemistry of cyanoselenoacetamide, Chem. Heterocycl. Comp. 49 (5) (2013) 657–675.
[27] J. Rafique, S. Saba, R.F.S. Canto, T.E.A. Frizon, W. Hassan, E.P. Waczuk, M. Jan, D.F. Back, J.B.T. Da Rocha, A.L. Braga, Synthesis and biological evaluation of 2-picolylamide-based diselenides with non-bonded interactions, Molecules 20 (6) (2015) 10095–10109.
[28] Y. Liang, Y. Zhou, S. Deng, T. Chen, Microwave-assisted syntheses of benzimidazole-containing selenadiazole derivatives that induce cell-cycle arrest and apoptosis in human breast cancer cells by activation of the ROS/AKT pathway, Chem. Med. Chem. 11 (20) (2016) 2339–2346.
[29] T. Cierpiał, J. Łuczak, M. Kwiatkowska, P. Kiełbasiński, L. Mielczarek, K. Wiktorska, Z. Chilmonczyk, M. Milczarek, K. Karwowska, Organofluorine isoselenocyanate analogues of sulforaphane: synthesis and anticancer activity, Chem. Med. Chem. 11 (21) (2016) 2398–2409.
[30] M.F.B. Gerzson, F.N. Victoria, C.S. Radatz, M.G. de Gomes, S.P. Boeira, R.G. Jacob, D. Alves, C.R. Jesse, L. Savegnago, In vitro antioxidant activity and in vivo antidepressant-like effect of α-(phenylselanyl) acetophenone in mice, Pharmacol. Biochemis. Behav. 102 (1) (2012) 21–29.
[31] L. Carroll, D.I. Pattison, S. Fu, C.H. Schiesser, M.J. Davies, C.L. Hawkins, Catalytic oxidant scavenging by selenium-containing compounds: reduction of selenoxides and N-chloramines by thiols and redox enzymes, Redox Biol. 12 (2017) 872–882.
[32] S. Shaaban, E. Gaffer, M. Alshahd, S.S. Elmorsy, Cytotoxic symmetrical thiazole diselenides with increased selectivity against MCF-7 breast cancer cells, Int. J. Res. Develop. Pharm. Life Sci 4 (2015) 1654–1668.
[33] I. Ingold, C. Berndt, S. Schmitt, S. Doll, G. Poschmann, K. Buday, A. Roveri, X. Peng, F.P. Freitas, T. Seibt, Selenium utilization by GPX4 is required to prevent

hydroperoxide-induced ferroptosis, Cell 172 (3) (2018) 409–422. e21.
[34] Y.A. Ivanenkov, M.S. Veselov, I.G. Rezekin, D.A. Skvortsov, Y.B. Sandulenko, M.V. Polyakova, D.S. Bezrukov, S.V. Vasilevsky, M.E. Kukushkin, A.A. Moiseeva, Synthesis, isomerization and biological activity of novel 2-selenohydantoin derivatives, Bioorgan. Med. Chem. 24 (4) (2016) 802–811.
[35] H. Wójtowicz, K. Kloc, I. Maliszewska, J. Młochowski, M. Piętka, E. Piasecki, Azaanalogues of ebselen as antimicrobial and antiviral agents: synthesis and properties, Il Farmaco 59 (11) (2004) 863–868.
[36] M.E. Khalifa, S.H. Abdel-Hafez, A.A. Gobouri, M.I. Kobeasy, Synthesis and biological activity of novel arylazothiazole disperse dyes containing selenium for dyeing polyester fibers, Phosphorus Sulfur Silicon Relat. Elem. 190 (4) (2015) 461–476.
[37] F. Cisnetti, A. Gautier, Metal/N-heterocyclic carbene complexes: opportunities for the development of anticancer metallodrugs, Angew. Chem. Int. Ed. 52 (46) (2013) 11976–11978.
[38] M.A. Iqbal, R.A. Haque, W.C. Ng, L.E.H. Hassan, A.M.S.A. Majid, M.R. Razali, Green synthesis of mono- and di-selenium-N-heterocyclic carbene adducts: characterizations, crystal structures and pro-apoptotic activities against human colorectal cancer, J. Organomet. Chem. 801 (2016) 130–138.
[39] M.A. Iqbal, R.A. Haque, S.F. Nasri, A.A. Majid, M.B.K. Ahamed, E. Farsi, T. Fatima, Potential of silver against human colon cancer:(synthesis, characterization and crystal structures of xylyl (Ortho, meta, & Para) linked bis-benzimidazolium salts and Ag (I)-NHC complexes: In vitroanticancer studies), Chem. Cent. J. 7 (1) (2013) 27.
[40] M.A. Iqbal, M.I. Umar, R.A. Haque, M.B.K. Ahamed, M.Z.B. Asmawi, A.M.S.A. Majid, Macrophage and colon tumor cells as targets for a binuclear silver (I) N-heterocyclic carbene complex, an anti-inflammatory and apoptosis mediator, J. Inorg. Biochem. 146 (2015) 1–13.
[41] R.A. Haque, M.A. Iqbal, P. Asekunowo, A.A. Majid, M.B.K. Ahamed, M.I. Umar, S.S. Al-Rawi, F.S.R. Al-Suede, Synthesis, structure, anticancer, and antioxidant activity of para-xylyl linked bis-benzimidazolium salts and respective dinuclear Ag (I) N-heterocyclic carbene complexes (Part-II), Med. Chem. Res. 22 (10) (2013) 4663–4676.
[42] R.A. Haque, S.Y. Choo, S. Budagumpi, M.A. Iqbal, A.A.-A. Abdullah, Silver (I) complexes of mono-and bidentate N-heterocyclic carbene ligands: synthesis, crystal structures, and in vitro antibacterial and anticancer studies, Eur. J. Med. Chem. 90 (2015) 82–92.
[43] R.A. Haque, N. Hasanudin, M.A. Hussein, S.A. Ahamed, M.A. Iqbal, Bis-N-heterocyclic carbene silver (I) and palladium (II) complexes: Efficient antiproliferative agents against breast cancer cells, Inorg. Nano-Met. Chem. 47 (1) (2017) 131–137.
[44] M.A. Iqbal, R.A. Haque, W.C. Ng, L.E. Hassan, A.M. Majid, M.R. Razali, Green synthesis of mono-and di-selenium-N-heterocyclic carbene adducts: characterizations, crystal structures and pro-apoptotic activities against human colorectal cancer, J. Organomet. Chem. 801 (2016) 130–138.
[45] R.A. Haque, M.A. Iqbal, F. Mohamad, M.R. Razali, Antibacterial and DNA cleavage activity of carbonyl functionalized N-heterocyclic carbene-silver (I) and selenium compounds, J. Mole. Struct. 1155 (2018) 362–370.
[46] I. Wiegand, K. Hilpert, R.E. Hancock, Agar and broth dilution methods to determine the minimal inhibitory concentration (MIC) of antimicrobial substances, Nat. Protocols 3 (2) (2008) 163–175.
[47] P.O. Asekunowo, R.A. Haque, Counterion-induced modulation in biochemical properties of nitrile functionalized silver (I)-N-heterocyclic carbene complexes, J. Coord. Chem. 67 (22) (2014) 3649–3663.
[48] R. Cao, H. Ji, N. Feng, Y. Zhang, X. Yang, P. Andersson, Y. Sun, K. Tritsaris, A.J. Hansen, S. Dissing, Collaborative interplay between FGF-2 and VEGF-C promotes lymphangiogenesis and metastasis, Proc. Natl. Acad. Sci. (2012) 201208324.
[49] K. Wang, J. Zheng, Signaling regulation of fetoplacental angiogenesis, J. Endocrinol. 212 (3) (2012) 243–255.
[50] K. Leahy, A. Koki, J. Masferrer, Role of cyclooxygenases in angiogenesis, Curr. Med. Chem. 7 (11) (2000) 1163–1170.
[51] X. Lv, J. Li, C. Zhang, T. Hu, S. Li, S. He, H. Yan, Y. Tan, M. Lei, M. Wen, The role of hypoxia-inducible factors in tumor angiogenesis and cell metabolism, Genes Diseases 4 (1) (2017) 19–24.
[52] K. Mandal, S.B. Kent, Total chemical synthesis of biologically active vascular endothelial growth factor, Angew. Chemie Int. Ed. 50 (35) (2011) 8029–8033.
[53] S. Jiang, L. Zhang, D. Cui, Z. Yao, B. Gao, J. Lin, D. Wei, The important role of halogen bond in substrate selectivity of enzymatic catalysis, Sci. Rep. 6 (2016) 34750.
[54] A. Kahraman, R.J. Morris, R.A. Laskowski, A.D. Favia, J.M. Thornton, On the diversity of physicochemical environments experienced by identical ligands in binding pockets of unrelated proteins, Proteins: Struct. Funct. Bioinformatics 78 (5) (2010) 1120–1136.
[55] M. Egli, S. Sarkhel, Lone pair − aromatic interactions: to stabilize or not to stabilize, Acc. Chem. Res. 40 (3) (2007) 197–205.
[56] S. Fang, L. Li, B. Cui, S. Men, Y. Shen, X. Yang, Structural insight into plant programmed cell death mediated by BAG proteins in Arabidopsis thaliana, Acta Crystallogr. Sect. D: Biol. Crystallogr. 69 (6) (2013) 934–945.